

# Structure and Allostery of the Chaperonin GroEL

Helen R. Saibil<sup>1</sup>, Wayne A. Fenton<sup>2</sup>, Daniel K. Clare<sup>1</sup> and Arthur L. Horwich<sup>2,3</sup>

**1 - Crystallography and Institute of Structural and Molecular Biology, Birkbeck College London, Malet Street, London WC1E 7HX, UK**

**2 - Department of Genetics, Yale University School of Medicine, 295 Congress Avenue, New Haven CT 06510, USA**

**3 - Howard Hughes Medical Institute, Yale University School of Medicine, 295 Congress Avenue, New Haven CT 06510, USA**

**Correspondence to Arthur L. Horwich:** [arthur.horwich@yale.edu](mailto:arthur.horwich@yale.edu)

<http://dx.doi.org/10.1016/j.jmb.2012.11.028>

**Edited by C. Kalodimos**

## Abstract

Chaperonins are intricate allosteric machines formed of two back-to-back, stacked rings of subunits presenting end cavities lined with hydrophobic binding sites for nonnative polypeptides. Once bound, substrates are subjected to forceful, concerted movements that result in their ejection from the binding surface and simultaneous encapsulation inside a hydrophilic chamber that favors their folding. Here, we review the allosteric machine movements that are choreographed by ATP binding, which triggers concerted tilting and twisting of subunit domains. These movements distort the ring of hydrophobic binding sites and split it apart, potentially unfolding the multiply bound substrate. Then, GroES binding is accompanied by a 100° twist of the binding domains that removes the hydrophobic sites from the cavity lining and forms the folding chamber. ATP hydrolysis is not needed for a single round of binding and encapsulation but is necessary to allow the next round of ATP binding in the opposite ring. It is this remote ATP binding that triggers dismantling of the folding chamber and release of the encapsulated substrate, whether folded or not.

The basis for these ordered actions is an elegant system of nested cooperativity of the ATPase machinery. ATP binds to a ring with positive cooperativity, and movements of the interlinked subunit domains are concerted. In contrast, there is negative cooperativity between the rings, so that they act in alternation. It is remarkable that a process as specific as protein folding can be guided by the chaperonin machine in a way largely independent of substrate protein structure or sequence.

© 2012 Elsevier Ltd. All rights reserved.

## Introduction

Nature's use of allosteric action in proteins was first elegantly articulated for a set of four proteins in the classic publication of Monod *et al.* 50 years ago.<sup>1</sup> With the exception of Perutz' early structure of hemoglobin,<sup>2</sup> showing the heme groups to be distant from each other and to change distance upon oxygenation, Monod *et al.* had little structural information on which to rest their model, despite its clear dependence on structural changes driven by allosteric effectors. These pioneers could probably never have imagined the spectacular panoply of both enzymes and molecular machines that are recognized today to employ allosteric action to carry out their biological functions.

Surely ranking among the more interesting allosteric proteins is the chaperonin GroEL, a protein folding

machine, first identified<sup>3,4</sup> some years after the classic allostery paper and intensively studied over four decades. Here, we focus on the structural nature of the allosteric action of this double-ring machine, particularly on the action of ATP. ATP is an allosteric ligand for GroEL, its binding promoting both cooperative (intra-ring) and anti-cooperative (inter-ring) actions.<sup>5</sup> In addition, ATP serves as a substrate, undergoing hydrolysis during the reaction cycle<sup>6</sup> to promote a unidirectional advance of the machine.<sup>7,8</sup> Before focusing on the allosterically driven structural changes, we introduce the quaternary and domain architecture that are the subject of allosteric action, review the overall action of the machine in assisting protein folding as directed by such allosterically driven movements, and briefly review biochemical observations describing the allosteric behavior.

## Quaternary and Domain Architecture of GroEL Disposing to Allosteric Behavior

Consistent with the early speculations of Monod *et al.* concerning quaternary structure of cooperative proteins,<sup>1</sup> GroEL is composed of multiple identical protomers, 14 in all, arranged in a symmetric fashion as two back-to-back seven-member rings (Fig. 1a and b).<sup>9</sup> The rotational symmetry of the rings is readily appreciable in end views (Fig. 1b), but there is also symmetry between rings, involving seven 2-fold symmetry axes between subunits in the apposing rings, producing an overall symmetry of D7. Each GroEL protomer (57 kDa) is composed of two major domains, an equatorial domain at the waistline of the cylinder and an apical domain at the terminal end, covalently connected by a smaller intermediate domain that is hinged at its top and bottom aspects to allow for rigid-body movements (Fig. 1c). Each

equatorial domain houses an ATP binding pocket,<sup>11</sup> and seven of these domains contact each other side by side in each ring. The two rings contact each other back to back in a staggered fashion across the equatorial plane (Fig. 1a), forming a platform on which the other two domains of the machine undergo major movements in response to ATP binding and hydrolysis.<sup>12,13</sup> The equatorial domains themselves also undergo subtle cooperative movements during the reaction cycle,<sup>14</sup> responsible for the asymmetric behavior of the machine, dictating that only one ring is folding active at a time.

The other major domain is the apical domain, lying at the terminal end of the cylinder and containing a hydrophobic surface exposed to solvent at the cavity-facing aspect,<sup>9,15</sup> lying ~40 Å from the equatorial ATP binding pocket. This is the polypeptide-binding surface, denoted by red and orange helices H and I and an underlying segment

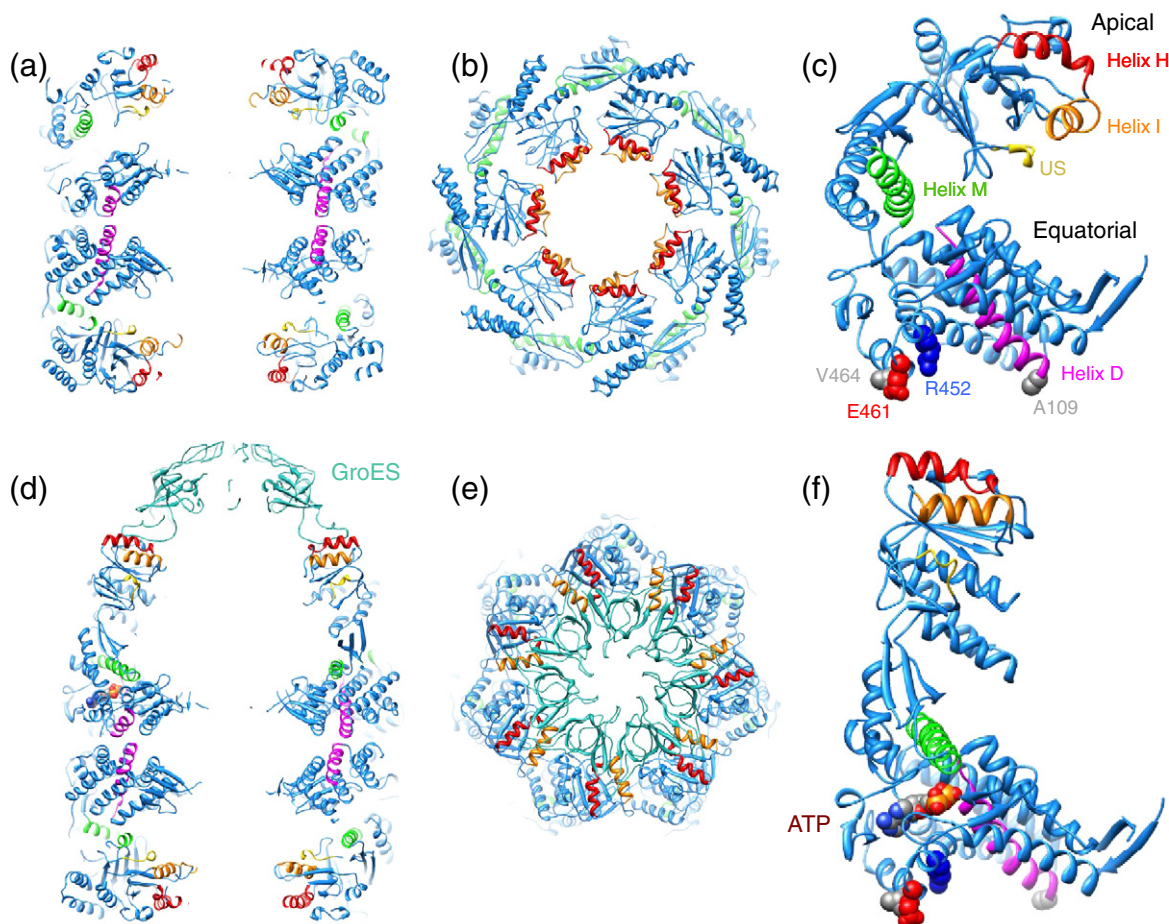


**Fig. 1.** X-ray crystal structures of GroEL and GroEL–GroES complexes. (a) Central side view slice through the GroEL 14-mer [Protein Data Bank (PDB) code 1OEL]<sup>9</sup> showing the two back-to-back rings. (b) End view of a GroEL ring, seen from outside the complex. (c) A GroEL subunit, seen in approximately the same orientation as the top left subunit in (a). The apical and equatorial domains are labeled, as are helix H (red), helix I (orange), underlying segment (US; yellow), helix M (green), helix D (magenta), along with the residues forming the inter-ring contacts (E461, R452, V464, and A109). (d–f) Equivalent views of the GroEL–GroES–ATP complex (PDB code 1SVT),<sup>10</sup> including the cochaperonin lid GroES [blue green (d and e)] and the bound nucleotide (f).

(yellow). The seven apical domains of an open GroEL ring form a smooth hydrophobic surface with which to selectively capture nonnative polypeptides via their own exposure of hydrophobic surfaces that will be buried in the interior in the native state.<sup>16,17</sup>

Finally, the small intermediate domain allows for hinged movements at its top and bottom aspects (Fig. 1c), enabling at the bottom aspect the intermediate domain to rotate down onto the ATP pocket, bringing with it the base (Asp398) that activates a water to mediate ATP hydrolysis,<sup>10,13</sup> and allowing at the top aspect the apical domains to open via elevation and twisting movements (Fig. 1d–f).<sup>14</sup> The movements of the intermediate and apical domains, and of the machine in general, are rigid-body movements, greatly facilitating the analysis of the machine in free solution by electron microscopy (EM), obviating the constraints of a crystal lattice. Rigid-body fitting of intermediate states observed by cryo-EM has been carried out using X-ray data from the two states that have been captured crystallographically, the unliganded state (Fig. 1a–c)<sup>9</sup> and the cochaperonin (GroES)-bound state (Fig. 1d–f),<sup>13</sup> comprising essentially the end-state structures of GroEL rings.

### GroEL Uses Its Apical Domains and Central Cavity, Remote from the ATP Binding Pocket, to Supply Kinetic Assistance to Polypeptide Folding

In a polypeptide binding-proficient state, the collective of apical domains of a ring provides, as mentioned, a hydrophobic surface on which a nonnative substrate is multivalently captured in the open ring; that is, the collapsed substrate polypeptide is bound by multiple surrounding apical domains.<sup>16,17</sup> Other portions of larger substrate proteins can protrude out of the central cavity like a champagne cork.<sup>18</sup>

Under physiological conditions, there is an order of events to convert a ring of an unliganded GroEL complex to a folding-active state: ATP binds rapidly to a ring (<20 ms), followed by polypeptide binding (20–200 ms), followed by binding the cochaperonin lid protein GroES (~200 ms) (see Ref. 19 for a review). GroES, itself a seven-membered homo-oligomeric ring (composed of ~10-kDa subunits and overall resembling a “lid”),<sup>20</sup> makes 1:1 contacts with subunits of an ATP-bound GroEL ring, proffering from each GroES subunit a mobile loop that has a hydrophobic edge, IVL, to make contact with the hydrophobic surface of a corresponding ATP-mobilized apical domain of a GroEL subunit (Fig. 1d–f).<sup>10,13</sup> Following initial contact with GroES (~200 ms), a point at which both nonnative polypeptide and GroES are simultaneously bound to the apical domains, large, forceful, and cooperative

rigid-body rotations of the apical domains lead to release of polypeptide substrate from the cavity wall into a now GroES-capped central cavity.<sup>10,14,21</sup> During these rigid-body movements, the hydrophobic binding surface that initially captured the polypeptide is removed from facing the cavity (by virtue of apical domain elevation and clockwise rotation) and is replaced with a hydrophilic, richly electrostatic (net negatively charged) lining.<sup>10,13</sup> The released polypeptide then folds in solitary confinement in this domed chamber, using the information in its primary structure to direct proper folding,<sup>22,23</sup> as first articulated by Anfinsen. We view the walls of this chamber, albeit physically close to the folding substrate protein and subject to collisions with it,<sup>24</sup> as a “non-stick” surface that effectively allows folding to occur as if at infinite dilution. Indeed, for a number of substrate proteins where the rate of folding to native form has been compared under so-called “permissive” conditions (lower temperature or lower substrate protein concentration, enabling spontaneous folding to occur in solution), the rate of folding inside the chamber is similar to that at high dilution in free solution.<sup>23,25</sup>

### Biochemical and Mutational Observations of Allosteric Behavior

Cooperativity in GroEL was first detected by ATP hydrolysis measurements of Gray and Fersht,<sup>26</sup> and a Hill coefficient of 1.86 was calculated. Further analyses from several laboratories have confirmed this, with general agreement on a Hill coefficient of about 2.5 (in the absence of GroES).<sup>27,28</sup> Gray and Fersht also noted that the presence of GroES reduced the rate of hydrolysis by ~50%, while increasing the Hill coefficient to 3.<sup>26</sup> This established GroES as an allosteric effector of ATP hydrolysis. Further observations of asymmetry of both nucleotide and GroES binding<sup>29–32</sup> led to a suggestion that there is negative cooperativity between GroEL rings, and this was established by the kinetic work of Yifrach and Horovitz,<sup>5</sup> who developed the following model of nested cooperativity.<sup>33</sup> Within a ring, there is a concerted Monod–Wyman–Changeux model operative,<sup>34</sup> such that a ring is in equilibrium between a T state (low affinity for ATP) and an R state (high affinity for ATP). This implies that ATP binds preferentially to the R ring and hence shifts the equilibrium toward the high-affinity R state. A second level of cooperativity was proposed to apply between the two rings and follows the Koshland–Nemethy–Filmore model of sequential transition (TT→TR→RR).<sup>35</sup> Fitting initial rates of ATP hydrolysis across a concentration range, Yifrach and Horovitz observed the two transitions, with a Hill coefficient of 2.75 for the concerted intraring T→R step and 0.003 for the second sequential step. The observation of a Hill coefficient <1

indicates that the inter-ring transition occurs with negative cooperativity.

Fluorescence changes were also monitored by Yifrach and Horovitz using a variant GroEL with equatorial residue F44 changed to tryptophan (wild-type GroEL is devoid of tryptophan).<sup>36</sup> Stopped-flow mixing of ATP with GroEL showed a fast phase with bi-sigmoidal dependence on ATP concentration, and mathematical analysis yielded the same binding constants and Hill coefficients as had been observed earlier. Two slow phases were also observed, and one was assigned to ATP hydrolysis.

Slower phases following addition of ATP to tryptophan-modified GroELs have also been observed by Cliff *et al.* (equatorial Y485W)<sup>37</sup> and Taniguchi *et al.* (apical R231W).<sup>38</sup> These studies also revealed a rapid early phase of fluorescence

enhancement ( $t_{1/2} < 20$  ms). Because the apical reporter, W231, reported this same phase, presumably the early conformational change exerted by ATP association in the equatorial domains is transmitted to the apical domains. A second phase of fluorescence quenching was reported on a timescale of 200 ms,<sup>37,38</sup> likely corresponding to apical elevation and counterclockwise twisting movements, which will be discussed below. This phase likely accommodates polypeptide binding because GroES forms an initial association with GroEL, closing access to the central cavity, only at the end of this phase. A subsequent third phase of tryptophan fluorescence quenching of W485 (enhancement of W231) is affected by GroES (producing further quench of W485)<sup>37,38</sup> and corresponds to a phase where a prebound fluorescent substrate

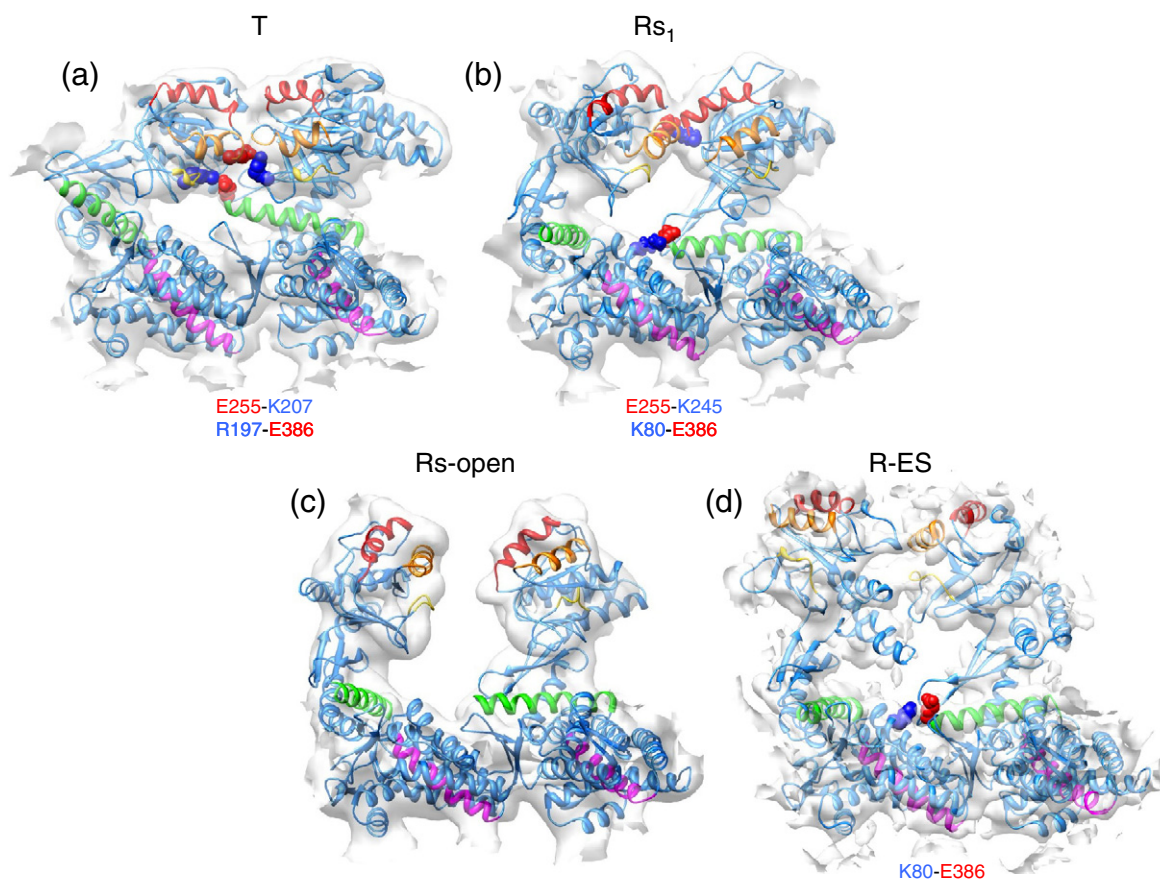


**Fig. 2.** Two adjacent subunits seen from inside the GroEL ring, showing the cryo-EM maps and fitted atomic structures of the subunit domains for four major GroEL conformations. The color coding is as in Fig. 1. Intersubunit salt-bridge residues are shown as spheres colored by charge (red, negative; blue, positive). (a) T state (unliganded) GroEL. The two initial salt bridges are R197–E386 and E255–K207. (b) The GroEL-ATP<sub>7</sub> state Rs<sub>1</sub>. The two original salt bridges are replaced by K80–E386 and E255–K245. An en bloc movement of the intermediate and apical domains has partly closed helix M (green) over the nucleotide pocket and has tilted the apical domains, leaving a distorted band of hydrophobic sites lining the inside of the cavity. (c) In the GroEL-ATP<sub>7</sub> Rs-open state, the apical domains are elevated and the ring is radially expanded so that the intersubunit contacts, including the salt bridges, are lost, but helix I and underlying segment sites still face individually into the cavity. (d) When GroES (not shown) binds, the apical domains come back into contact after a 100° excursion, which fully removes the hydrophobic sites from the cavity-facing surface. The intersubunit K80–E386 salt bridge reforms in this state. Maps EMD 1997, 1998, 2000, and 1180; PDB codes 4AAQ, 4AAS, and 2C7C.<sup>14,39</sup> Panels a-c are modified from Fig. 4 of ref. 14.

(fluorescent-labeled RCMLA) underwent changes suggestive of release into the GroES-encapsulated chamber.<sup>37</sup> Thus, a sequence of allosterically driven events in a ring is directed by the binding of ATP to that ring, preceding the hydrolysis of ATP.

By contrast with the foregoing events in the ring to which ATP is bound (i.e., in *cis* to ATP), the arrival of ATP drives the rapid allosteric discharge of GroES and folding polypeptide from the opposite (*trans*) ring (<1 s).<sup>7,8</sup> That is, at the same time that ATP binding nucleates a folding reaction in the ring to which it binds, it sends signals that discharge the ligands in the opposite ring. Notably, the GroES being discharged lies >100 Å away from the ATP binding site.

Mutations have been made in a number of individual GroEL residues to test their roles in allosteric communication. Most have been evaluated *in vitro* with respect to ATP binding and hydrolysis, while a few have also been tested *in vitro* or *in vivo* for their effects on protein folding. The earliest studied such mutation, R197A, destroys a vital intersubunit salt bridge (with residue E386 in the intermediate domain; see Fig. 2 and section below).<sup>5</sup> Both positive and negative cooperativity are reduced, with the result that the T→R transitions in both rings occur at lower ATP concentrations. The structural consequences of this mutation have been addressed with a low-resolution (30 Å) cryo-EM reconstruction,<sup>40</sup> which showed a “loosening” of the rings, likely due to releasing the salt-bridge constraints that hold the rings in the T state until full occupancy with ATP is achieved. Another early variant was the double mutant, R13G/A126V, which was the GroEL form initially crystallized.<sup>9</sup> Although this variant is functional *in vivo*, negative cooperativity is abolished while positive cooperativity remains intact.<sup>41</sup> This suggests that these changes in the equatorial domain disrupt inter-ring communication, although a more detailed analysis has not been carried out. Mutations in residues that have been predicted to interact during allosteric transitions have also been studied, both singly and in pairs. For example, changes to both members of one pair, E409–R501, which form an inter-domain salt bridge, between the pivot point of helix M and the equatorial domain of the same subunit, resulted primarily in decreased positive cooperativity.<sup>42</sup> The energetics of the T→R transitions in these mutants were interpreted to reflect that the salt bridge was weakened during ATP-driven allosteric movements, although it did not appear to be broken.

An interesting mutation, D155A, of a residue involved in an intra-subunit salt bridge, D155–R395, also affected positive cooperativity, such that the normally concerted T→R transition of one ring was replaced by a sequential (or partially sequential) transition at low ATP concentrations.<sup>43</sup> Structurally, the D155–R395 salt bridge is near the intersubunit R197–E386 one (E386 and R395 are both on helix

M), and the authors suggested that breaking the former one weakens the latter and permits the relative stabilization of intermediates in the allosteric transition in which only three or four subunits have undergone the T→R switch. This interpretation of the kinetics was supported by single-particle reconstructions from negative-stain EM images obtained with low concentrations of ATP that produced image classes with apparent breaks in the symmetry of a ring. It also should be noted that the affected salt bridge is near residue D398, which is critically involved in positioning a water molecule required for ATP hydrolysis adjacent to the  $\gamma$ -phosphate of ATP.<sup>10,13</sup> The effect of this change from a concerted to a sequential switch has been examined *in vitro* using artificial, chimeric substrates.<sup>44</sup> Refolding of both domains of a CyPet–YPet chimera with D155A showed a bi-sigmoidal dependence on ATP concentration, compared with a mono-sigmoidal dependence with wild-type GroEL.<sup>44</sup> These data were interpreted to mean that the sequential ATP-dependent allosteric switch in the mutant led to a sequential release of the substrate protein, while the concerted switch in wild type produced concerted substrate release and folding. The authors concluded that the concerted switch is important for GroEL's biological function.<sup>44</sup>

Some of the foregoing mutations have been tested *in vivo*, and most are compatible with growth of *E. coli* at normal temperatures, although a few are temperature sensitive (e.g., R197A; also see discussion of E461K below). When tested, their ability to support protein folding *in vitro* appears to be substrate dependent and also depends on whether GroES is required for the folding reaction.<sup>45</sup>

## Allosteric Structural Changes in an ATP-Bound GroEL Ring

A recent cryo-EM study, using a hydrolysis-defective GroEL mutant, D398A, able to bind ATP with normal affinity but hydrolyzing at a rate ~2% normal, has simultaneously captured three states of an ATP-bound ring that likely form a trajectory of movement beyond the T state toward the fully GroES-bound state (Fig. 2).<sup>14</sup> For this study, rapid freezing was employed after ATP mixing. Resolution was at the level of 8–9 Å. Although these states coexist in solution and are presumably in equilibrium with each other, they can be ordered into a clear trajectory showing progressive movements. The first state beyond the T state, called Rs<sub>1</sub>, is produced by a cooperative en bloc movement of both the intermediate and apical domains, involving a 35° sideways tilting of the intermediate and apical domains as a single rigid-body unit about the lower hinge of the intermediate domain. This acts to rotate the intermediate domain (including the long  $\alpha$  helix

M, shown in green) down into the equatorial ATP binding pocket, bringing the catalytic D398 residue into the pocket, where it forms a number of hydrogen bonds.<sup>10,13</sup> Attendant to this movement, a unique salt bridge between the intermediate domain of one subunit and the apical domain of its clockwise neighbor (in end-on view), E386–R197, is broken and is replaced by a new salt bridge between E386 in the intermediate domain and K80 in the neighboring equatorial domain. This reflects the downward movement of the intermediate domain. At the same time, an apical–apical salt bridge, K207–E255 between neighboring subunits (helix I–underlying segment; see diagram of the three-tiered apical cavity-facing structure in Fig. 1c), is broken and replaced by a new K245–E255 bridge (helix H–helix I), reflecting the en bloc tilting movement.<sup>14</sup>

A second state, called  $Rs_2$ , is produced by a small additional rigid-body elevation of the apical domains at the top hinge of the intermediate domain. The various salt bridges of  $Rs_1$  are retained at this step. The third state,  $Rs$ -open, is produced next, when the apical domains move radially outward and elevate a further 20° (Fig. 2). This breaks the apical salt bridges and effectively liberates the apical domains from each other. Separation of the apical domains could potentially unfold a misfolded substrate polypeptide. The  $Rs$ -open state is the only one in which domains can move independently, and one or two apical domains may elevate before the others. Yet their hydrophobic polypeptide binding surfaces remain facing the central cavity (in the absence of any substantial twisting motion). Importantly, the outward radial motion of the hydrophobic surface places it in a position to directly align with the hydrophobic mobile loops of GroES, enabling an initial contact with the cochaperonin and ending the polypeptide binding phase of the reaction cycle. All of this takes place in ~200–300 ms.

In the absence of an experiment that could time-dependently capture the individual ATP-driven states, one can only speculate that  $Rs_1$  corresponds to the rapid fluorescent phase that reflects initial ATP binding where, indeed, apical changes have been reported by Taniguchi *et al.*<sup>38</sup>  $Rs$ -open would correspond to the phase at which GroES contact has an effect on the amplitude of the fluorescence signal of reporters in the kinetics experiments of Cliff *et al.*<sup>37</sup> and Taniguchi *et al.*<sup>38</sup>

The question remains as to how the various movements are programmed by the binding of ATP in the equatorial pocket. One could speculate that there are thermal fluctuations that can populate the  $Rs_1$  state even in the absence of ATP and that ATP binding simply stabilizes this state by hydrogen-bonding interactions (e.g., between D398 and nucleotide bound in the ATP binding pocket). The nature of the subsequent further apical elevation and the outward radial motion with attendant breakage of salt bridges—50 Å away from the pocket—remains

unclear. A model of electrostatic “click-stops”, that is, progressive salt bridge replacements during upward apical movement on the way to complete salt bridge breakage, could suggest that the stops represent local energetic minima on a landscape whose ultimate minimum is the fully opened and freed apical domains. On the other hand, the finding of three states at once in the cryo-EM study might imply that all three of the states lie on a fairly shallow energy landscape and that there could be backward transitions from  $Rs$ -open to  $Rs_2$  to  $Rs_1$  in the absence of GroES. It could be that the docking of GroES stabilizes the  $Rs$ -open state, taking this assembly to a more energetically stable state that is no longer reversible and that is committed to the further large movements to a final energetic minimum that is the fully domed end state.

### GroES Contact Leads to Large Rigid-Body Apical Movements That Eject Polypeptide into an Enclosed Folding Chamber

Following GroES contact, the subsequent step of further apical domain elevation and 100° clockwise twist to produce the folding-active GroES-domed state of GroEL (R-ES) occurs over ~1 s, attended by forceful release of substrate protein into the *cis* folding chamber.<sup>21,37,38</sup> The cooperative nature of these movements of the apical domains is likely enforced by the 7-fold occupancy of ATP and the 7-fold symmetry of the GroEL ring.<sup>46</sup> The subunit domains cannot move independently without steric collision except upon reaching the  $Rs$ -open state where the apical domains are freed from each other. Because this state rapidly becomes bound and constrained by 7-fold symmetric GroES, such independent mobility is likely to be short lived. ATP is absolutely required for the step of polypeptide release that occurs following GroES collision during the large rigid-body movements that form the folding chamber.<sup>10</sup> Interestingly, while ADP will support formation of the full domed conformation in the presence of GroES, it will not lead to ejection of substrate proteins from the cavity wall.<sup>10,21,24</sup> Remarkably, however, addition of ground-state or transition-state metal complexes,  $BeF_x$  or  $AlF_3$ , respectively, to such an ADP-bound complex will drive productive release of polypeptide from the walls of *cis* ADP complexes with subsequent production of the native state in the *cis* chamber.<sup>10</sup> Thus, the binding of the  $\gamma$ -phosphate moiety of ATP in the seven equatorial pockets can effectively provide the energy needed (~40 kcal/mol rings) to allosterically eject polypeptide from the cavity walls. The nature of this action, for example, whether a further transient clockwise twist of the apical domains occurs, as might be suggested by observation of a fluorescent transient,<sup>21</sup> is unknown.

In sum, the final elevation and twist of the apical domains (following initial GroES contact) that triggers *cis* folding is crucially dependent on cooperative ATP binding in the seven equatorial pockets and on

GroES contacting the apical domains. On GroEL's own energy landscape, these movements take the machine to a stable energetic minimum that is the folding-active state.

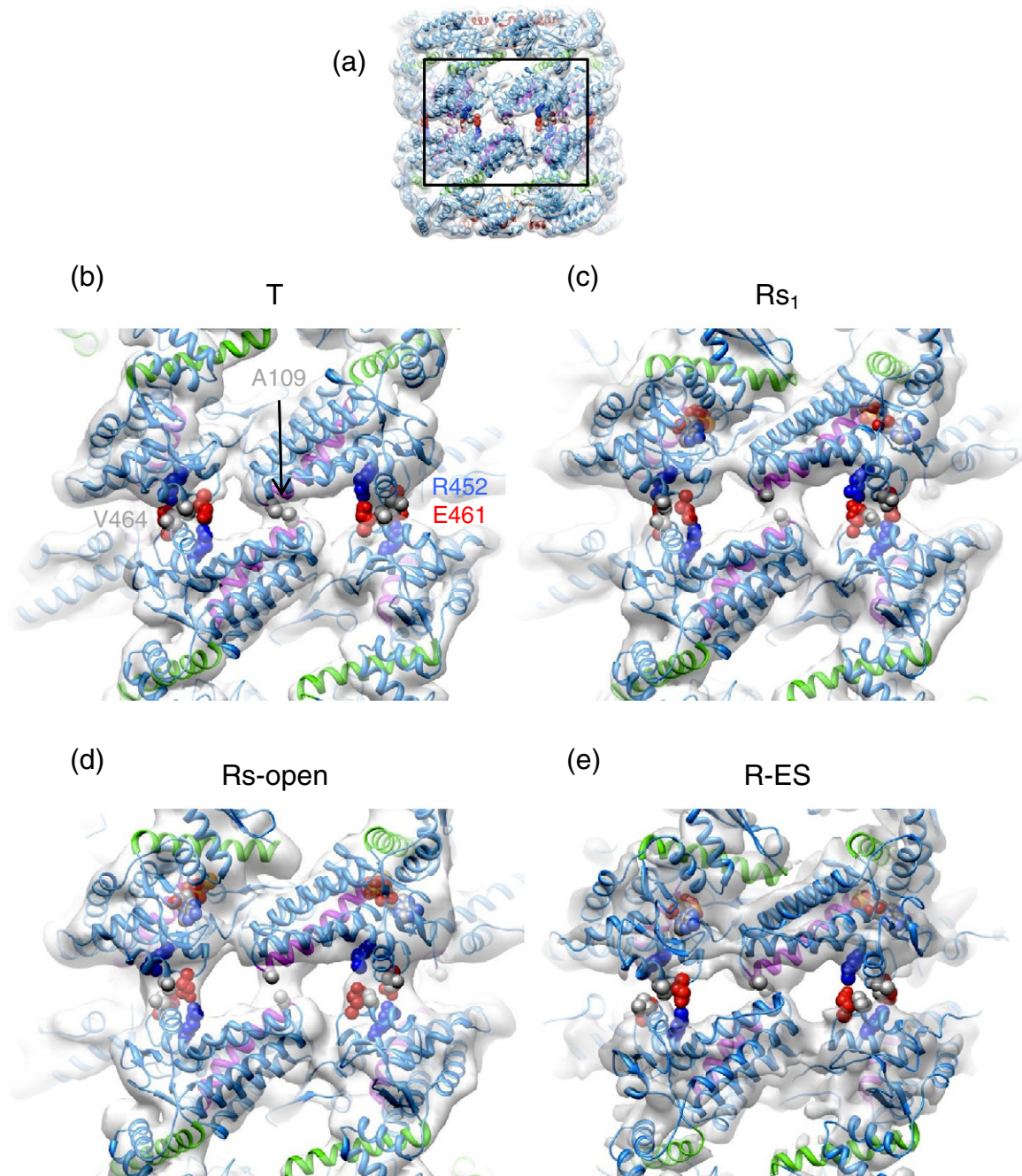


**Fig. 3.** Inter-ring contacts in the ATPase cycle. (a) Overview indicating the region displayed in (b) to (f). (b) Inter-ring interface of the T state viewed from outside the complex. The key residues forming the two contacts are shown as spheres. R452 (red) and E461 (blue) form salt bridges, and the residues A109 (gray) at the end of helix D (magenta) form a hydrophobic contact. (c) View of the interface in the Rs<sub>1</sub> state, where a tilt of the equatorial domains in the ATP-bound ring weakens the A109–A109 contact. (d) In the Rs-open state, the A109–A109 contact is further expanded. (e) In the R-ES state (GroEL–GroES–ATP<sub>7</sub>), the interface is partly restored toward the conformation of the T state, but the contacts are somewhat weaker, with a slightly different orientation of the equatorial domains in the *trans* (lower) ring. Citations and structure files are as in Fig. 2. Modified from Fig. 5 of ref. 14.

## Structural Basis of Negative Cooperativity between Rings

The two GroEL rings, as mentioned, are staggered in their back-to-back positioning, such that each subunit harbors two points of contact, symmetrically contacting the same sites in two adjacent subunits of the opposite ring (Fig. 3a). One site involves a symmetric interaction of E461/R452/V464 in the subunit of one ring with the same site in a subunit of the opposite ring, while the other involves an A109–A109 symmetric contact between the subunit of one ring and those residues in the neighboring subunit in the opposite ring.<sup>9</sup> Notably, A109 lies at the distal end of helix D (magenta), which extends from the nucleotide pocket, and this contact is thus a likely direct transducer of the state of nucleotide occupancy at the pocket of one ring through the corresponding D helix in a subunit of the opposite ring to its nucleotide pocket. Binding of ATP, in addition to producing the changes described above in intermediate and apical domains of the ring to which it binds, also causes significant equatorial movements in the bound ring.<sup>14,39</sup> These amount to pivoting the equatorial domains about the 461–452–464 contact such that the 109–109 contact is both lengthened (by 2 Å) and changed from a tilted to a more vertical orientation (Fig. 3). The lengthening seems likely to account for

the negative cooperativity between rings for ATP binding, possibly through alteration of electrostatic interactions between the apposed D helices by the presence of the  $\gamma$ -phosphate.<sup>39</sup> These movements, occurring as a result of the ATP-dependent pivoting, result in a more globally observable counterclockwise rotation (looking in end view) and expansion of the entire ATP-bound ring (Fig. 4, Rs<sub>1</sub> and Rs-open). The transition at the inter-ring interface involves, on one hand, a tilt of the equatorial domain centered on the 461–452–464 contact that widens the A109–A109 distance and, on the other, a counterclockwise rotation of the whole ATP-bound ring of equatorial domains relative to the unoccupied state.<sup>14</sup>

These ATP-triggered conformational changes prime the subsequent states of GroES binding. The twist between equatorial rings remains very similar in the ATP bullet complex (GroEL–ATP–GroES), although it is accompanied by the additional changes in domain tilt and ring separation described above. Only upon ATP hydrolysis, as inferred from the structure of the ADP bullet, is the twist reversed.

## Action of ATP Hydrolysis in Release of *cis* Ligands

Examination of equatorial domain rings in the ATP and ADP bullet complexes suggests that ATP

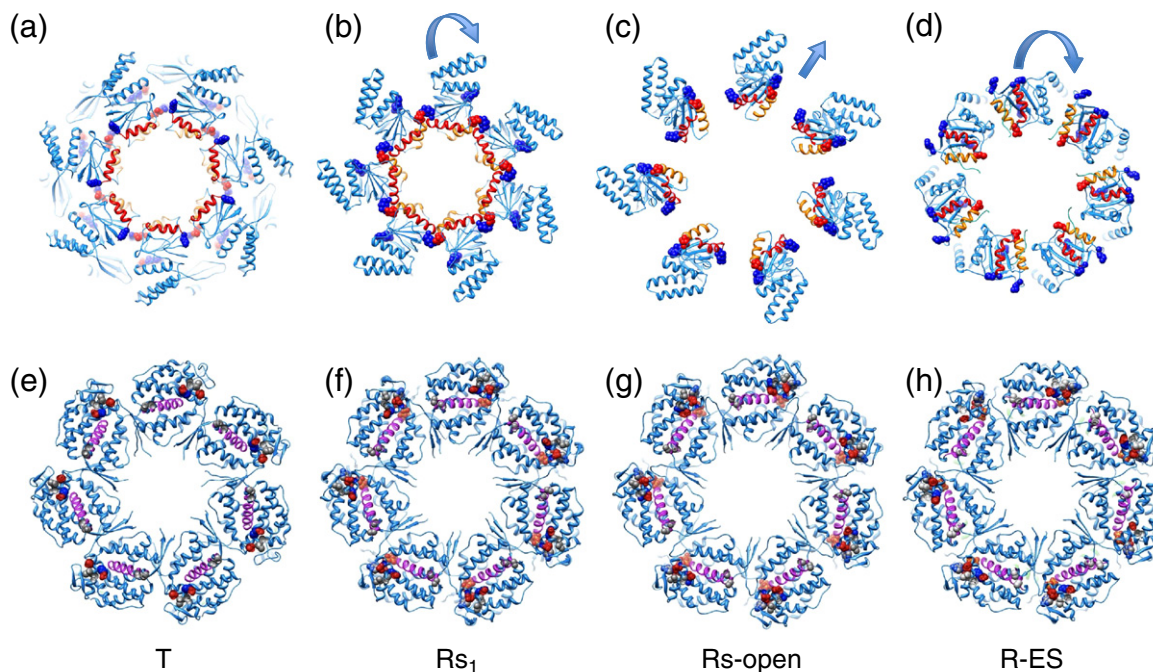


**Fig. 4.** Subunit rotations in the apical and equatorial domains. (a–d) Views of the apical domains of a ring from outside the complex, showing the distortion of the T state ring by tilting of the apical domains in the Rs<sub>1</sub> state, their separation and elevation in the Rs-open state, and the complete occlusion of the substrate binding sites by a 100° rotation to the R-ES state. (e–h) Views of the *cis* equatorial domains of a ring seen from the ring interface for the same four states. The T state ring is distorted by a small rotation of each domain in Rs<sub>1</sub> and a radial expansion in Rs-open and restored to the T state conformation in R-ES. Citations and structure files are as in Fig. 2.

hydrolysis in *cis* produces a strained conformation in the resulting ADP bullet.<sup>39</sup> This ADP state is primed to release the *cis* ligands, that is, GroES, nucleotide, and polypeptide substrate, by opening the *cis* folding chamber. The main distortion, unique to the ADP bullet state, is an opening of the  $\beta$ -sheet contact between equatorial domains within the *trans* ring (Fig. 5).<sup>14,39</sup> This is a key contact holding the rings together; hence, the ADP bullet must be a less stable state of the complex. The *trans* ring of the ADP bullet rapidly binds ATP, which then triggers the release of GroES and opening of the *cis* chamber. We hypothesize that the conformational change triggered by ATP binding in *trans* restores the  $\beta$ -sheet contacts, thus making the interface incompatible with the *cis* bullet conformation, so that GroES is

released and the complex is reset. An illustration of this allosteric coupling was provided by a temperature-sensitive GroEL mutant in the key salt bridge between the rings, E461K.<sup>47–49</sup> Remarkably, this mutant forms a rearranged assembly with a 1:1 subunit contact instead of 1:2 across the ring interface (Fig. 6). Even more surprisingly, this complex is functional at permissive temperatures, but loses function at 37 °C because the rings dissociate and GroES release is impaired.<sup>48</sup> The loss of inter-ring coupling at the non-permissive temperature is presumably because the alternative 1:1 interface is not stabilized by any salt bridges,<sup>49</sup> unlike the wild type that is held together by E461–R452. It is interesting to note that in group II chaperonins, the corresponding sequence provides

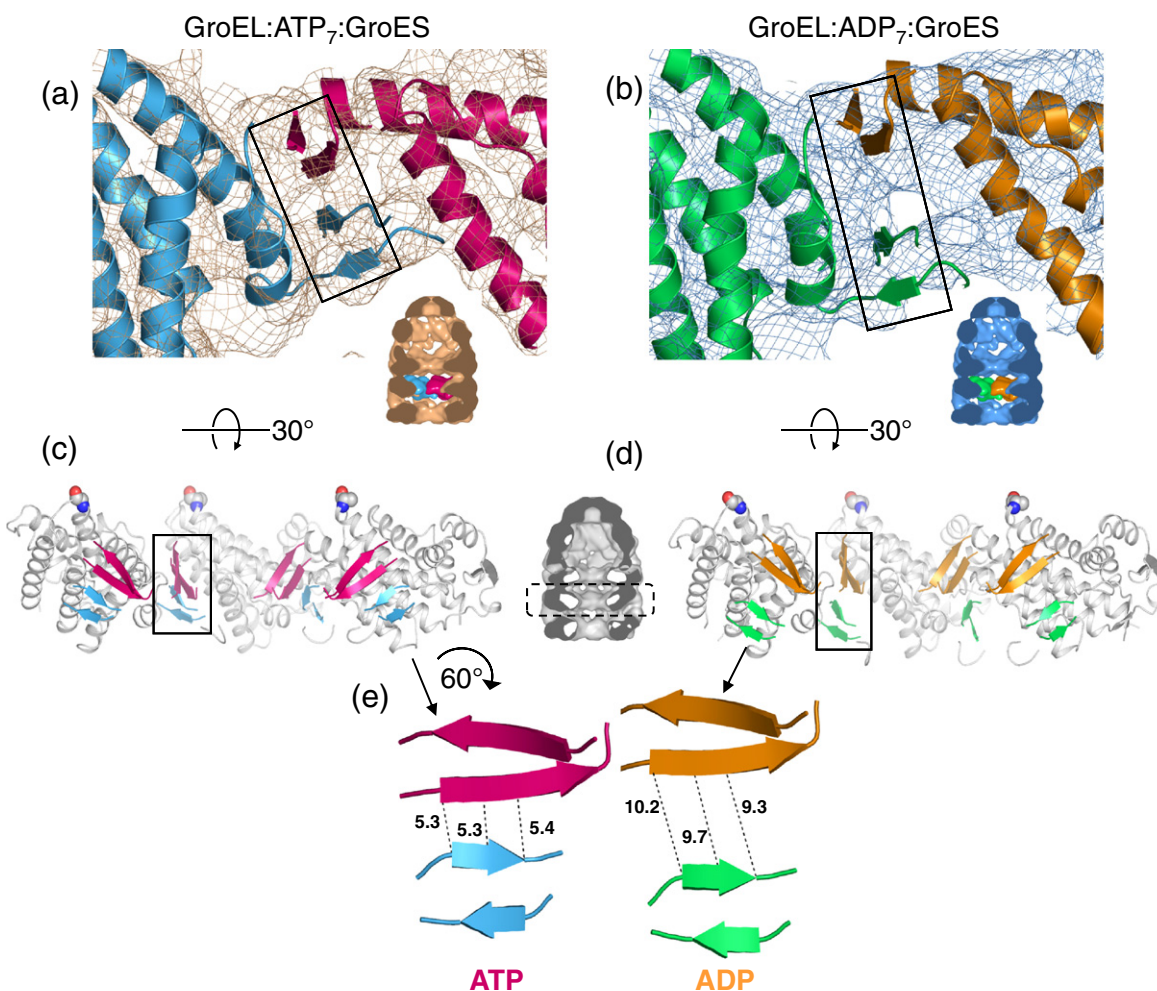


**Fig. 5.** Opening of the intersubunit  $\beta$ -sheet contact in the *trans* ring after ATP hydrolysis in the GroEL–GroES complex. (a) The  $\beta$ -sheet contact between N- and C-terminal regions of adjacent equatorial domains in a *trans* ring. The cryo-EM map is shown in gold mesh and the rigid-body fitted domains are shown in contrasting colors for the two adjacent subunits. (b) In the ADP complex, the cryo-EM map (blue mesh) shows a clear separation at this contact site, arising from tilts of the equatorial domains. (c and d) View of the  $\beta$ -sheets from inside the ring in the fitted atomic models of the ATP and ADP complexes. (e) Inter-strand distances from the atomic model. The figure was reproduced from Ref. 39 with permission from Macmillan Publishers, Ltd: *Nature Structural and Molecular Biology*, copyright 2006. Maps EMD 1180 and 1181; PDB codes 2C7C and 2C7D.

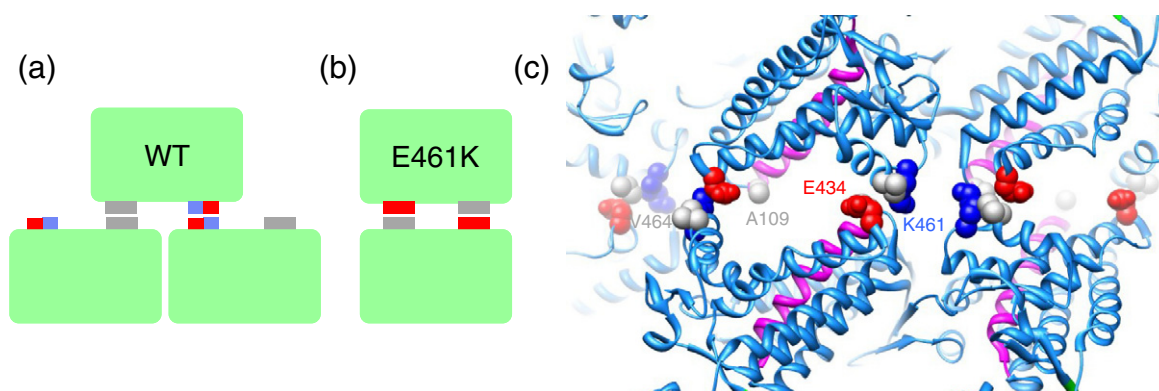


**Fig. 6.** The E461K mutant of GroEL has a rearranged inter-ring interface. Schematic models of the wild type (WT) and E461K interfaces show how the normal 1:2 contacts of apposed equatorial domains in wild-type GroEL are replaced by 1:1 contacts in the mutant. The atomic structure of the interface is illustrated by a view from the outside of the crystal structure of this mutant (PDB code 2EU1).<sup>49</sup> The 3.3-Å structure suggests that there are no salt bridges stabilizing this interface and that the single type of contact involves K461, V464, and E434. A109 does not make any inter-ring contact in the mutant assembly.

salt bridge contacts at the 1:1 positions.<sup>50</sup> The result of nucleotide and GroES binding to E461K GroEL is a dead-end single ring–GroES complex such as SR1. It is clear from the effects of this and other mutations that the structure of the ring interface is closely coupled to GroES binding.

## Summary of Current Understanding

As exemplified by the nonfunctional E461K mutant discussed above, allosteric actions not just within the GroEL rings but between them are crucial to the operation of the machine. The allosteric changes that we have just discussed, both within and between rings, are summarized schematically in Fig. 7. ATP is the major driver, acting upon binding within a ring to

direct a trajectory of cooperative rigid-body movements during the first ~200 ms to produce the Rs<sub>1</sub> and Rs-open states to which substrate polypeptide binds (Fig. 7b and c). At the end of that time, polypeptide is likely encapsulated by the collision of GroES with Rs-open, forming a ternary complex in which both the substrate protein and the GroES mobile loops simultaneously occupy parts of the apical hydrophobic binding surface. This is followed by large, forceful, and cooperative rigid-body elevations and 100° clockwise twisting movements of the apical domains of the *cis* ring, while it remains associated with GroES, which occur over the subsequent second to produce the domed GroEL:ATP<sub>7</sub>:GroES folding chamber (Fig. 7d). Polypeptide substrate is released from the cavity wall during this large and forceful excursion and proceeds to fold. At the same time ATP drives these

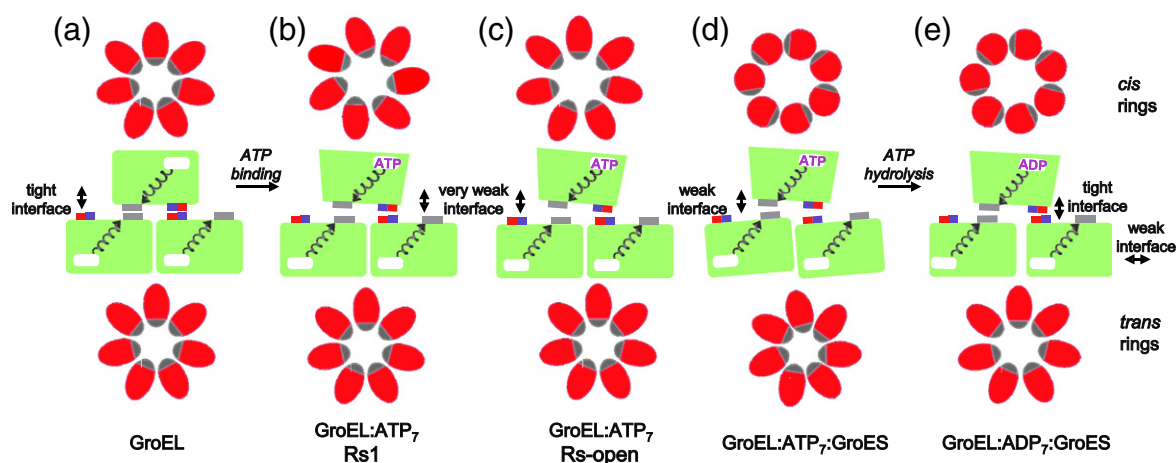


**Fig. 7.** Schematic diagrams of allosteric domain movements in GroEL complexes. The apical domains (*cis* on top, *trans* on bottom) are represented by red ellipses or circles, with gray regions indicating the hydrophobic binding sites, and the equatorial domains are represented by green rectangles, with the inter-ring contacts residues as blue, red, or gray boxes. Helix D is shown schematically running from the ATP binding pocket (white rectangle) to the A109 contact (gray boxes).

events in the *cis* ring, it also acts through equatorial helix D and the 461–452 contacts between the rings to effectively “shut off” the opposite ring, disfavoring binding of ATP (and thus GroES) there, as well as disfavoring binding of nonnative substrate protein. The subsequent hydrolysis of ATP in the *cis* ring after ~10 s (Fig. 7e) then “resets” the equatorial contacts (associated with the splaying of the *trans* ring equatorial intersubunit  $\beta$ -sheet) and gates entry of ATP into the *trans* ring (with reformation of the  $\beta$ -sheet). Newly bound ATP once again acts through helix D to disturb the 109–109 interface and sends long-range signals that eject GroES, polypeptide, and ADP from what had been the folding-active ring. The nature of the ring adjustments at the apical and intermediate domain levels that leads to departure of GroES (and ADP) remains unknown. Concerning GroES release, one can speculate that a reversed movement of the apical domains, in the counterclockwise direction, would break the contacts of the mobile loops with the apical domains. Regardless, this movement is occurring 100 Å from the *trans* ring ATP signal and comprises but one of the remarkable allosterically driven steps of this machine that awaits understanding.

## Acknowledgements

A.L.H. would like to thank the Howard Hughes Medical Institute for its long-standing support of his lab's structural and biochemical investigations of chaperonin function. H.R.S. thanks the Wellcome Trust for long-term programme and equipment grant support.

Received 1 November 2012;

Received in revised form 19 November 2012;

Accepted 20 November 2012

Available online 24 November 2012

### Keywords:

molecular chaperone;  
allostery

## References

1. Monod, J., Changeux, J.-P. & Jacob, F. (1963). Allosteric proteins and cellular control systems. *J. Mol. Biol.* **6**, 306–329.
2. Perutz, M. F., Rossmann, M. G., Cullis, A. F., Muirhead, H., Will, G. & North, A. C. (1960). Structure of haemoglobin: a three-dimensional Fourier synthesis at 5.5-Å resolution, obtained by X-ray analysis. *Nature*, **185**, 416–422.
3. Georgopoulos, C. P., Hendrix, R. W., Kaiser, A. D. & Wood, W. B. (1972). Role of the host cell in bacteriophage morphogenesis: effects of a bacterial mutation on T4 head assembly. *Nat. New Biol.* **239**, 38–41.
4. Takano, T. & Kakefuda, T. (1972). Involvement of a bacterial factor in morphogenesis of bacteriophage capsid. *Nat. New Biol.* **239**, 34–37.
5. Yifrach, O. & Horovitz, A. (1994). Two lines of allosteric communication in the oligomeric chaperonin GroEL are revealed by the single mutation Arg196→Ala. *J. Mol. Biol.* **243**, 397–401.
6. Chandrasekhar, G. N., Tilly, K., Woolford, C., Hendrix, R. & Georgopoulos, C. (1986). Purification and properties of the groES morphogenetic protein of *Escherichia coli*. *J. Biol. Chem.* **261**, 12414–12419.
7. Rye, H. S., Burston, S. G., Fenton, W. A., Beechem, J. M., Xu, Z., Sigler, P. B. & Horwich, A. L. (1997). Distinct actions of *cis* and *trans* ATP within the double ring of the chaperonin GroEL. *Nature*, **388**, 792–798.
8. Rye, H. S., Roseman, A. M., Chen, S., Furtak, K., Fenton, W. A., Saibil, H. R. & Horwich, A. L. (1999). GroEL–GroES cycling: ATP and nonnative polypeptide direct alternation of folding-active rings. *Cell*, **97**, 325–338.
9. Braig, K., Otwinowski, Z., Hegde, R., Boisvert, D. C., Joachimiak, A., Horwich, A. L. & Sigler, P. B. (1994). The crystal structure of the bacterial chaperonin GroEL at 2.8 Å. *Nature*, **371**, 578–586.
10. Chaudhry, C., Farr, G. W., Todd, M. J., Rye, H. S., Brunger, A. T., Adams, P. D. *et al.* (2003). Role of the  $\gamma$ -phosphate of ATP in triggering protein folding by GroEL–GroES: function, structure and energetics. *EMBO J.* **22**, 4877–4887.
11. Boisvert, D. C., Wang, J., Otwinowski, Z., Horwich, A. L. & Sigler, P. B. (1996). The 2.4 Å crystal structure of the bacterial chaperonin GroEL complexed with ATP $\gamma$ S. *Nat. Struct. Biol.* **3**, 170–177.
12. Roseman, A. M., Chen, S., White, H., Braig, K. & Saibil, H. R. (1996). The chaperonin ATPase cycle: mechanism of allosteric switching and movements of substrate-binding domains in GroEL. *Cell*, **87**, 241–251.
13. Xu, Z., Horwich, A. L. & Sigler, P. B. (1997). The crystal structure of the asymmetric GroEL–GroES–(ADP) $\gamma$  chaperonin complex. *Nature*, **388**, 741–750.
14. Clare, D. K., Vasishtan, D., Stagg, S., Quispe, J., Farr, G. W., Topf, M. *et al.* (2012). ATP-triggered conformational changes delineate substrate-binding and -folding mechanics of the GroEL chaperonin. *Cell*, **149**, 113–123.
15. Fenton, W. A., Kashi, Y., Furtak, K. & Horwich, A. L. (1994). Residues in chaperonin GroEL required for polypeptide binding and release. *Nature*, **371**, 614–619.
16. Farr, G. W., Furtak, K., Rowland, M. B., Ranson, N. A., Saibil, H. R., Kirchhausen, T. & Horwich, A. L. (2000). Multivalent binding of nonnative substrate proteins by the chaperonin GroEL. *Cell*, **100**, 561–573.
17. Elad, N., Farr, G. W., Clare, D. K., Orlova, E. V., Horwich, A. L. & Saibil, H. R. (2007). Topologies of a substrate protein bound to the chaperonin GroEL. *Mol. Cell*, **26**, 415–426.
18. Thiyagarajan, P., Henderson, S. J. & Joachimiak, A. (1996). Solution structures of GroEL and its complex with rhodanese from small-angle neutron scattering. *Structure*, **4**, 79–88.

19. Horwich, A. L. & Fenton, W. A. (2009). Chaperonin-mediated protein folding: using a central cavity to kinetically assist polypeptide chain folding. *Q. Rev. Biophys.* **42**, 83–116.
20. Hunt, J. F., Weaver, A. J., Landry, S. J., Gierasch, L. & Deisenhofer, J. (1996). The crystal structure of the GroES co-chaperonin at 2.8 Å resolution. *Nature*, **379**, 37–45.
21. Motojima, F., Chaudhry, C., Fenton, W. A., Farr, G. W. & Horwich, A. L. (2004). Substrate polypeptide presents a load on the apical domains of the chaperonin GroEL. *Proc. Natl Acad. Sci. USA*, **101**, 15005–15012.
22. Apetri, A. C. & Horwich, A. L. (2008). Chaperonin chamber accelerates protein folding through passive action of preventing aggregation. *Proc. Natl Acad. Sci. USA*, **105**, 17351–17355.
23. Tyagi, N. K., Fenton, W. A., Deniz, A. A. & Horwich, A. L. (2011). Double mutant MBP refolds at same rate in free solution as inside the GroEL/GroES chaperonin chamber when aggregation in free solution is prevented. *FEBS Lett.* **585**, 1969–1972.
24. Weissman, J. S., Rye, H. S., Fenton, W. A., Beechem, J. M. & Horwich, A. L. (1996). Characterization of the active intermediate of a GroEL–GroES-mediated protein folding reaction. *Cell*, **84**, 481–490.
25. Hofmann, H., Hillger, F., Pfeil, S. H., Hoffmann, A., Streich, D., Haenni, D. *et al.* (2010). Single-molecule spectroscopy of protein folding in a chaperonin cage. *Proc. Natl Acad. Sci. USA*, **107**, 11793–11798.
26. Gray, T. E. & Fersht, A. R. (1991). Cooperativity in ATP hydrolysis by GroEL is increased by GroES. *FEBS Lett.* **292**, 254–258.
27. Jackson, G. S., Staniforth, R. A., Halsall, D. J., Atkinson, T., Holbrook, J. J., Clarke, A. R. & Burston, S. G. (1993). Binding and hydrolysis of nucleotides in the chaperonin catalytic cycle—implications for the mechanism of assisted protein folding. *Biochemistry*, **32**, 2554–2563.
28. Horovitz, A., Bochkareva, E. S., Kovalenko, O. & Girshovich, A. S. (1993). Mutation Ala2→Ser destabilizes intersubunit interactions in the molecular chaperone GroEL. *J. Mol. Biol.* **231**, 58–64.
29. Bochkareva, E. S., Lissin, N. M., Flynn, G. C., Rothman, J. E. & Girshovich, A. S. (1992). Positive cooperativity in the functioning of molecular chaperone GroEL. *J. Biol. Chem.* **267**, 6796–6800.
30. Burston, S. G., Ranson, N. A. & Clarke, A. R. (1995). The origins and consequences of asymmetry in the chaperonin reaction cycle. *J. Mol. Biol.* **249**, 138–152.
31. Saibil, H., Dong, Z., Wood, S. & auf der Mauer, A. (1991). Binding of chaperonins. *Nature*, **353**, 25–26.
32. Langer, T., Pfeifer, G., Martin, J., Baumeister, W. & Hartl, F. U. (1992). Chaperonin-mediated protein folding: GroES binds to one end of the GroEL cylinder, which accommodates the protein substrate within its central cavity. *EMBO J.* **11**, 4757–4765.
33. Yifrach, O. & Horovitz, A. (1995). Nested cooperativity in the ATPase activity of the oligomeric chaperonin GroEL. *Biochemistry*, **34**, 5303–5308.
34. Monod, J., Wyman, J. & Changeux, J.-P. (1965). On the nature of allosteric transitions: a plausible model. *J. Mol. Biol.* **12**, 88–118.
35. Koshland, D. E., Jr, Némethy, G. & Filmer, D. (1966). Comparison of experimental binding data and theoretical models in proteins containing subunits. *Biochemistry*, **5**, 365–385.
36. Yifrach, O. & Horovitz, A. (1998). Transient kinetic analysis of adenosine 5′-triphosphate binding-induced conformational changes in the allosteric chaperonin GroEL. *Biochemistry*, **37**, 7083–7088.
37. Cliff, M. J., Limpkin, C., Cameron, A., Burston, S. G. & Clarke, A. R. (2006). Elucidation of steps in the capture of a protein substrate for efficient encapsulation by GroE. *J. Biol. Chem.* **281**, 21266–21275.
38. Taniguchi, M., Yoshimi, T., Hongo, K., Mizobata, T. & Kawata, Y. (2004). Stopped-flow fluorescent analysis of the conformational changes in the GroEL apical domain. *J. Biol. Chem.* **279**, 16368–16376.
39. Ranson, N. A., Clare, D. K., Farr, G. W., Houldershaw, D., Horwich, A. L. & Saibil, H. R. (2006). Allosteric signaling of ATP hydrolysis in GroEL–GroES complexes. *Nat. Struct. Mol. Biol.* **13**, 147–152.
40. White, H. E., Chen, S., Roseman, A. M., Yifrach, O., Horovitz, A. & Saibil, H. R. (1997). Structural basis of allosteric changes in the GroEL mutant Arg197→Ala. *Nat. Struct. Biol.* **4**, 690–694.
41. Aharoni, A. & Horovitz, A. (1996). Inter-ring communication is disrupted in the GroEL mutant Arg13→Gly; Ala126→Val with known crystal structure. *J. Mol. Biol.* **258**, 732–735.
42. Aharoni, A. & Horovitz, A. (1997). Detection of changes in pairwise interactions during allosteric transitions: coupling between local and global conformational changes in GroEL. *Proc. Natl Acad. Sci. USA*, **94**, 1698–1702.
43. Danziger, O., Rivenzon-Segal, D., Wolf, S. G. & Horovitz, A. (2003). Conversion of the allosteric transition of GroEL from concerted to sequential by the single mutation Asp-155→Ala. *Proc. Natl Acad. Sci. USA*, **100**, 13797–13802.
44. Papo, N., Kipnis, Y., Haran, G. & Horovitz, A. (2008). Concerted release of substrate domains from GroEL by ATP is demonstrated with FRET. *J. Mol. Biol.* **380**, 717–725.
45. Yifrach, O. & Horovitz, A. (2000). Coupling between protein folding and allostery in the GroE chaperonin system. *Proc. Natl Acad. Sci. USA*, **97**, 1521–1524.
46. Ma, J. & Karplus, M. (1998). The allosteric mechanism of the chaperonin GroEL: a dynamic analysis. *Proc. Natl Acad. Sci. USA*, **95**, 8502–8507.
47. Horwich, A. L., Low, K. B., Fenton, W. A., Hirshfield, I. N. & Furtak, K. (1993). Folding in vivo of bacterial cytoplasmic proteins: role of GroEL. *Cell*, **74**, 909–917.
48. Sewell, B. T., Best, R. B., Chen, S., Roseman, A. M., Farr, G. W., Horwich, A. L. & Saibil, H. R. (2004). A mutant chaperonin with rearranged inter-ring electrostatic contacts and temperature-sensitive dissociation. *Nat. Struct. Mol. Biol.* **11**, 1128–1133.
49. Cabo-Bilbao, A., Spinelli, S., Sot, B., Agirre, J., Mechaly, A. E., Muga, A. & Guérin, D. M. (2006). Crystal structure of the temperature-sensitive and allosteric-defective chaperonin GroEL<sub>E461K</sub>. *J. Struct. Biol.* **155**, 482–492.
50. Ditzel, L., Lowe, J., Stock, D., Stetter, K. O., Huber, H., Huber, R. & Steinbacher, S. (1998). Crystal structure of the thermosome, the archaeal chaperonin and homologue of CCT. *Cell*, **93**, 125–138.